Surface kinetics of a nonlinear oxygen-induced (1×5)→(1×1) phase transition on Ir{100}

T. Ali, B. Klötzer, A. V. Walker, Q. Ge, and D. A. King

Citation: The Journal of Chemical Physics **109**, 9967 (1998); doi: 10.1063/1.477663
View online: http://dx.doi.org/10.1063/1.477663
View Table of Contents: http://scitation.aip.org/content/aip/journal/jcp/109/22?ver=pdfcov
Published by the AIP Publishing

Surface kinetics of a nonlinear oxygen-induced $(1\times5)\rightarrow(1\times1)$ phase transition on Ir{100}

T. Ali, B. Klötzer, A. V. Walker, Q. Ge, and D. A. King
Department of Chemistry, University of Cambridge, Lensfield Road, Cambridge CB2 1EW, United Kingdom

(Received 23 March 1998; accepted 3 September 1998)

The interaction of oxygen with the stable Ir{100}-(1×5) and the metastable (1×1) surfaces has been studied using supersonic molecular beams in the surface temperature range 200–1080 K. Starting from the clean (1×5) substrate, the adsorption kinetics are dominated by the adsorbate-induced lifting of the reconstruction. The formation of (1×1) islands occurs between two limiting oxygen surface coverages, as confirmed by helium scattering and low-energy electron diffraction (LEED) measurements. Two distinct temperature regimes are observed in the sticking probability measurements; between 350 and 600 K the local oxygen coverage on the (1×1) phase is about 0.28 monolayers (ML) during the prevailing phase transformation, whereas it is 0.20 ML in the temperature range 700–900 K. This ''biphasic'' behavior is explained by the enhancement of surface diffusion of adsorbed oxygen atoms at sample temperatures above 650 K and has been investigated further using thermal energy atom scattering (TEAS). In contrast to the (1×5) phase, TEAS measurements show that random adsorption of O_2 takes place on the clean metastable (1×1) surface. At 1080 K a pronounced flux dependence of the sticking probability is observed due to a nonlinear growth law for the formation of (1×1) islands, $r=c(\theta_O^{1\times5})^{4.5}$. Thermal desorption measurements accompanied by LEED show that the desorption rate is strongly influenced by the (1×1) to (1×5) surface phase transition; repulsive lateral interactions exist between adsorbed oxygen atoms on the (1×1) substrate. We present a mathematical model which takes these effects into account in reproducing the salient features of the temperature programmed desorption (TPD) spectra. Sticking probability, TEAS, and TPD data are all consistent with a defect concentration of 0.03 ML on the clean (1×5) surface annealed at 1400 K. © *1998 American Institute of Physics.* [S0021-9606(98)01546-3]

I. INTRODUCTION

The clean stable Ir{100} surface is reconstructed to a quasihexagonal top Ir atom layer (Fig. 1),[1–7] which is similar to the stable structures on Pt{100} or Au{100}. However, in contrast to Pt{100}, the thermodynamically stable structure exhibits an in-registry (1×5) low-energy electron diffraction (LEED) pattern due to a fit of the hexagonal layer to the substrate.[2,3] Adsorbate-free surfaces of both the metastable Ir{100}-(1×1) and the stable Ir{100}-(1×5) surfaces can be obtained under controlled experimental conditions.[2,3,6,8] In contrast to Pt{100}, the metastable (1×1) phase on Ir{100} is kinetically stable up to temperatures as high as 800 K.[2,3] Consistent with this, a recent theoretical study[9] revealed a high activation barrier for self-diffusion of Ir atoms on the Ir{100} surface. Dosing CO onto an Ir{100}-(1×5) surface causes local lifting of the (1×5) reconstruction, as shown by a recent molecular beam study carried out in our laboratory.[10]

There is little published work on oxygen adsorption on Ir surfaces of different orientations, but this does include LEED, photoemission spectroscopy, work function changes, and adsorption measurements.[4,6,11,12] A brief molecular beam study was focused on O_2 adsorption on Ir{110}-(1×2),[13] but there is no previous molecular beam study of O_2 adsorption on Ir{100}. The Ir{100}/O_2 system has been studied with thermal desorption spectroscopy (TDS), LEED, ultraviolet photoemission spectroscopy (UPS), and work function measurements, and marked chemical differences have been reported between the (1×1) and (1×5) surfaces with respect to oxygen adsorption.[4] A minimum amount of oxygen had to be adsorbed and a minimum annealing temperature of about 650 K had to be applied in order to establish a complete well-ordered Ir{100}-(1×1) substrate by oxygen adsorption.[4]

While the observation that adsorbates cause restructuring of solid surfaces is now widespread,[14] the study of the dynamics of these processes is still in its infancy. Recent studies of the kinetics of the adsorbate-induced restructuring of Pt{100}-hex to (1×1) by CO and D_2 adsorption[15,16] revealed a nonlinear growth law for the new phase,

$$r_{1\times1}=c\,\theta^n, \tag{1}$$

where $n\approx4$ and θ is the coverage of CO or D adatoms on the unreconstructed hex phase. The nonlinearity in the surface structural phase transition described by this power law plays a decisive role in the temporal oscillatory behavior of chemical reactions. The critical importance of the nonlinear term has already been shown for the oscillatory $CO+O_2$,[17] $CO+NO$,[18] and $NO+H_2$ [19] systems on Pt{100}. It was observed that even slight downward deviations of n from ~4 lead to a dampening or complete disappearance of the observed oscillatory behavior.

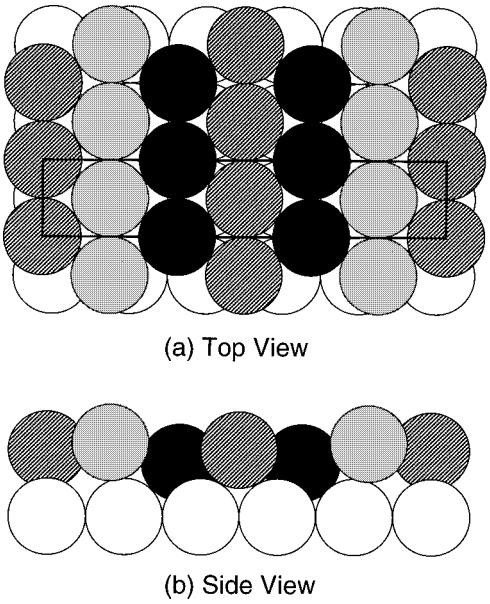

FIG. 1. The Ir {100}(1×5) structure. The top view shows the (1×5) (shaded circles) on top of the underlying (1×1) structure (open circles). The intensity of the shading in the top layer indicates the relative heights of these atoms.

Oxygen adsorption studies both on Pt{100}-hex and (1×1) showed a considerably higher initial dissociative sticking probability on the (1×1) than on the hex substrate. The formation of small oxygen-covered islands by random adsorption of immobile oxygen adatoms at 300 K was observed in the case of the hex surface, with a lifting of the local hex structure when the island size is $\geqslant$4.0 adatoms. On the (1×1) substrate no island formation took place.[20,21] Here we present an extension of these studies to Ir{100}-(1×5) and (1×1).

II. EXPERIMENT

In these experiments, a dual supersonic molecular beam system was used, which has been described previously.[15,20,22] The clean single-crystal Ir{100} surface (9 mm diam, 1.7 mm thick) was oriented within 0.5° of the bulk {100} plane and mechanically polished. Initially, the Ir{100} surface was cleaned by frequent cycles of prolonged Ar sputtering at 900 K, annealing at up to 1500 K, and oxygen treatment at 1160 K. Routine cleaning involved short occasional Ar sputtering at room temperature, followed by annealing at 1400 K, oxygen treatment at 1160 K, and finally flashing to 1400 K in vacuum. After this procedure the surface exhibited the reconstructed (1×5) LEED pattern with low background intensity and Auger electron spectroscopy showed impurities to be below the detection limit. A reproducible oxygen temperature programmed desorption (TPD) was obtained and a very intense specular He scattering signal pointed to a well annealed and clean surface. The clean unreconstructed (1×1) surface was prepared by the method described in Refs. 2 and 3. O_2 gas with a purity of 99.998 vol % (Messer UK Ltd.) was used in the adsorption experiments. For thermal energy atom scattering (TEAS) experiments during adsorption the oxygen was mixed with He in a 2 ℓ stainless steel mixing cylinder. Scattering measurements were performed using a high speed rotating chopper (75 Hz) in the second stage of the beam-forming chamber and a differentially pumped rotatable quadrupole mass spectrometer (QMS) which can perform angularly resolved line-of-sight detection of desorbing or directionally scattered species. Phase-lock techniques were employed to improve the signal-to-noise ratio and to reduce the QMS background signal in the scattering experiments. TEAS was used as a dynamic, nondestructive probe of O_a distribution and (1×1) island formation during the adsorbate-induced restructuring process. Only the intensity of the specular diffraction signal was monitored, as a function of exposure time, and no other (higher order) diffraction intensities were observed. TPD spectra and isothermal pressure curves were recorded by means of a second QMS in the main chamber, detecting a random flux of thermally desorbed molecules. For all TPD experiments a heating rate of 4 K/s was used. The coverage of adsorbed oxygen atoms is determined from the integral area of the TPD spectra and calibrated to the saturation oxygen coverage of 0.55 monolayers (ML) on the (1×1) substrate.

The TPD peak area of the oxygen saturation coverage, exhibiting a (2×2) LEED pattern described previously,[11] was calibrated by the following procedure. A saturated CO $c(2\times2)$ adlayer with a CO surface coverage of 6.6×10^{14} molecules/cm^2 (0.5 ML)[8] was dosed onto the clean metastable (1×1) surface. This adlayer was titrated using an O_2 beam of 0.025 ML/s at 480 K sample temperature and the resulting CO_2 peak was recorded. Conversely a saturated (2×2) adlayer of O(ad) was prepared by exposing the clean (1×1) surface at 800 K sample temperature (T_s) to an O_2 beam of 0.025 ML/s for up to 7 min. This adlayer was exposed to a room temperature CO beam (0.02 ML/s) at $T_s=650$ K and again the resulting CO_2 reaction peak was recorded. Several runs yielded almost equal or only slightly higher peak areas for the titration of preadsorbed oxygen, giving a saturation O coverage of 0.55 ML. This result is supported by a reported $p(2\times1)$O adlayer structure found after adsorption of NO up to saturation at 0.5 ML and desorption of nitrogen.[23] Further support comes from a $p(2\times1)$ oxygen adlayer on Pt{100}-(1×1) observed at 0.5 ML of O(ad) at low temperatures.[24]

Absolute (net) sticking probabilities as a function of exposure time were measured by the King and Wells beam reflectivity method,[25] and no corrections in the time-dependent pressure curve were necessary since the pumping speed during any experiment remained constant. Integration of the time-dependent pressure decrease due to sticking yields relative coverages versus time. All values for absolute fractional coverages are based on a surface Ir atom density of 1.32×10^{15} atoms/cm^2 of the metastable (1×1) surface. A calibration of the beam fluxes was derived from the ratio of absolute adsorption rate and the absolute sticking probability at the very beginning of the O_2 exposure and the result was compared with flux measurements obtained with a spinning rotor gauge.[26]

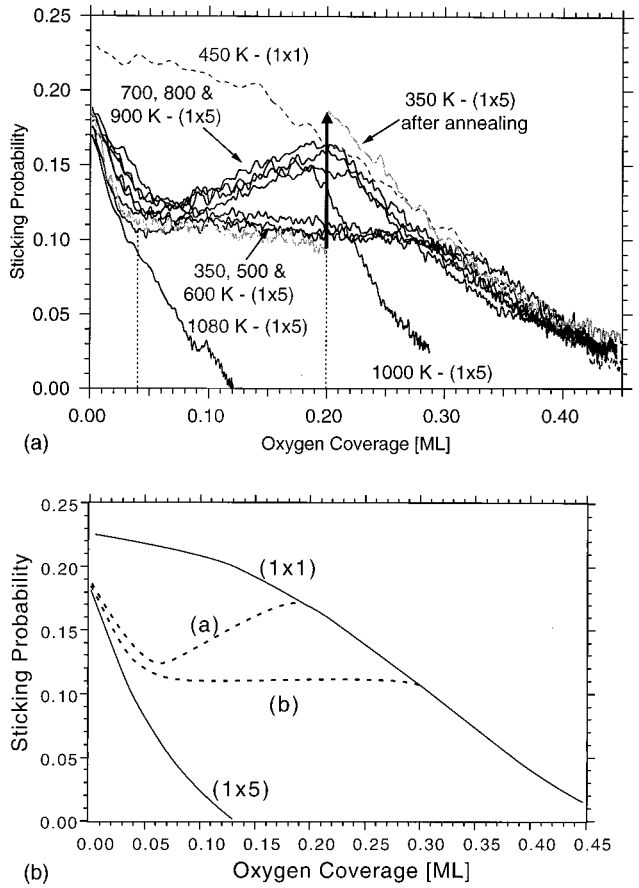

FIG. 2. (a) Absolute sticking probability vs oxygen coverage in the sample temperature range 350–1080 K. The beam flux for all experiments was 0.008 ML/s, the beam energy 0.06 eV. Black curves represent sticking on the (1×5) substrate and the dashed curve sticking on the metastable (1×1) substrate. The light grey curve represents a sticking experiment starting from the clean (1×5) surface at 350 K followed by intermediate annealing to 800 K at 0.20 ML mean oxygen coverage (thick arrow), followed by further uptake at 350 K up to saturation. The dashed vertical lines mark the coverage at which the phase transition starts and is completed at sample temperatures above 650 K. (b) Schematic representation clarifying the main features in (a).

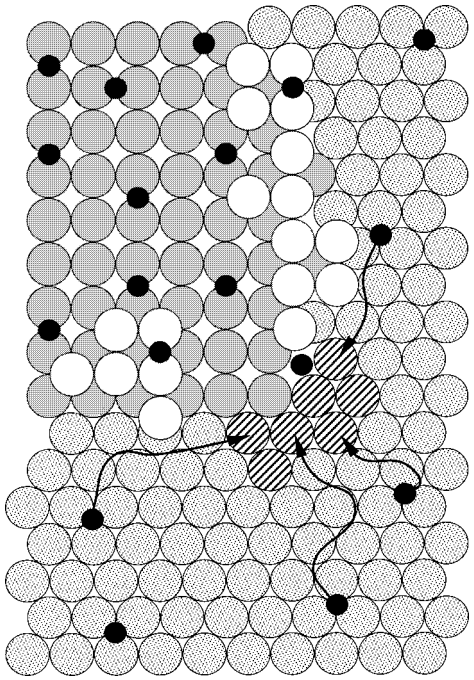

FIG. 3. A schematic illustration of the $(1\times5)\rightarrow(1\times1)$ phase transformation. Dotted circles represent surface iridium atoms in the (1×5) phase; grey circles represent Ir atoms in a growing (1×1) island; small black circles represent chemisorbed oxygen atoms, in the relative size corresponding to their covalent radius; open circles represent Ir atoms forced up as a result of the completed $(1\times5)\rightarrow(1\times1)$ phase transformation; hatched circles represent the next seven Ir atoms to be converted to (1×1) when four oxygen atoms from the (1×5) surface locally fluctuate toward the domain boundary.

III. RESULTS AND DISCUSSION

A. Sticking probability dependence on surface temperature and coverage

Figure 2(a) displays the experimental sticking probability dependence on oxygen coverage in the sample temperature range 350–1080 K at a flux of 0.008 ML/s and energy of 0.06 eV. Data were obtained from the metastable (1×1) surface, the reconstructed (1×5) surface, and during the (1×5) to (1×1) conversion. A simplified representation of the data is shown in Fig. 3. Here we note that the curve obtained at a substrate temperature of 450 K with an initial (1×1) surface corresponds, at coverages up to 0.45 ML of O adatoms, to adsorption on a (1×1) Ir{100} surface, while the curve obtained at 1080 K on an initially (1×5) surface corresponds to adsorption up to saturation—0.13 ML—on the (1×5) surface, i.e., without lifting the reconstruction. This is demonstrated later in Sec. III B and provides a simple key to understanding the remaining data, which involves the oxygen-induced switch of the Ir surface structure from (1×5) to (1×1).

On the initial (1×5) surface, the sticking probability for O_2 in the zero coverage limit is virtually independent of T_s, lying in the range 0.18 ± 0.01 for substrate temperatures between 350 and 1080 K. The absence of a significant dependence on T_s indicates that dissociative adsorption occurs on direct impact with the surface, without trapping into an intermediate molecular state. The rapid fall in sticking probability with increasing coverage on the (1×5) surface is also a strong indication of direct adsorption; at 1080 K this may be expected even for precursor-mediated adsorption, but we note that even at 450 K s falls rapidly with coverage in the range up to 0.05 ML, where no restructuring of the surface has occurred, as discussed below.

The saturation coverage achieved on the (1×5) surface at 1080 K—without lifting the reconstruction—is very low (0.12 ML) and deserves comment. At this temperature, once a significant coverage is achieved, the desorption rate becomes high, as shown in Sec. III D below. The measured zero sticking probability at 0.12 ML thus corresponds to an equilibration of adsorption and desorption rates: it is a *net* sticking. Nevertheless, the fall in sticking probability with coverage between 0 and 0.05 ML is very significant even at temperatures where desorption is insignificant. The conclusion, supported below, is that adsorption on the Ir{100}-(1×5) surface is dominated by defects, comprising as much as 5% of all surface sites.

On the metastable (1×1) surface at 450 K the initial sticking probability is 0.23, somewhat higher than on the

(1×5) surface, and the coverage dependence, which is only slight up to ~0.15 ML (Fig. 2), is *indicative* of precursor-mediated adsorption. All of the sticking probability data obtained at $\theta=0.27-0.45$ ML and $T_s=350-900$ K, are coincident with the data from an initial (1×1) clean surface. The result is surprising in view of the indication of precursor-mediated adsorption from the slow fall in s between 0 and 0.15 ML. At lower substrate temperatures the precursor should have a longer lifetime: at a given coverage, s should be higher at lower temperatures.[27] The behavior in the high coverage regime is therefore only consistent with direct adsorption. The data from the annealed surface at 350 K, the initial (1×1) clean surface, and at T_s between 700 and 900 K, all show a virtually linear fall with θ between 0.2 and 0.45 ML, extrapolating to zero at ~0.5 ML. We conclude that direct dissociative adsorption into a four site array is *not* blocked if one of the sites is filled with an adatom; but *is* blocked if two sites are occupied. This is an unusual, but not physically unreasonable, conclusion.

B. Sticking probabilities through the restructuring phase transition

The sticking probability results obtained from the initial (1×5) surface in the temperature range 350–1000 K are now readily attributed to a lifting of the (1×5) reconstruction over the coverage range from 0.05 to 0.28 ML at $T_s=350-600$ K, and from 0.05 to 0.20 ML at $T_s=700$ and 1000 K [Fig. 2(b)]. At all temperatures, island growth of the (1×1) phase is initiated at ~0.05 ML. In the high temperature regime, this is associated with a subsequent *increase* of s until a coverage of 0.20 ML is reached, when the s vs θ plot becomes identical to that of the initial (1×1) surface, suggesting that the (1×1) islands have coalesced at this coverage, with complete removal of the original (1×5) phase. If the local oxygen coverage on the (1×1) surface remains constant during island growth, this clearly suggests that it is ~0.2 ML, and the rising sticking probability is due to the greater activity of the (1×1) surface for oxygen sticking at 0.2 ML than the hex surface. In the lower substrate temperature range, 350–600 K, the $(1\times5)\rightarrow(1\times1)$ transformation occurs at constant sticking probability; the coalescence of growing islands occurs at 0.28 ML.

There are two growth regimes of the (1×1) phase as demonstrated in Fig. 2, with a sharp transition between regimes at between 600 and 700 K. We attribute this to the onset of rapid adatom diffusion in this temperature range. Earlier studies on Pt{100} provide a ready means of interpreting the present results; two related mechanisms for adsorbate-induced restructuring have been deduced.[15,16,20]

(i) With CO (and D), the hex to (1×1) transformation at temperatures between 380 and 450 K (200–240 K) is induced by *local density fluctuations* in the CO (D) adlayer, at very low coverages, on the hex phase.[15,16] When these fluctuations produce a local high density of adsorbed CO at the boundary of a growing (1×1)-CO island, or at a step, a patch of hex phase is converted to (1×1); the local density corresponds to four CO molecules covering about eight Pt surface atoms. This mechanism requires rapid diffusion of CO on the hex phase. A similar mechanism has recently been shown to take place for CO chemisorption on Ir{100}; the apparent local density of CO corresponds to a slightly larger value of about five molecules in this case.[10]

(ii) In contrast, for O_2 dissociative adsorption on Pt{100} at 300 K, the growth of the (1×1) phase is accompanied by a tenfold increase in the sticking probability, from 3×10^{-4} on the clean hex surface to $\sim3.7\times10^{-3}$ at $\theta=0.28$ ML. This rise is accompanied by the appearance of homogeneous nucleation of (1×1) islands.[28] Guo *et al.*[20] modeled the increasing sticking probability by assuming that the sticking probability at the edge of growing (1×1) islands was enhanced, and found that (a) nucleation of the (1×1) islands occurred when four C adatoms were adsorbed, by random collision from the gas phase, within a region of about eight surface Pt atoms on the hex phase. In this case the nucleation and growth of the islands proceeds within a *static* adsorbate layer on the hex phase.

We therefore conclude that in the temperature regime 700–1000 K the restructuring process is induced by local density fluctuations in the adlayer on the hex phase; the process on Ir {100} is schematically illustrated in Fig. 3. However, at lower temperatures the restructuring is induced within a static adlayer by statistically random dissociative adsorption. This conclusion is consistent with a *lower* local coverage (0.2 ML) within the growing (1×1) islands in the mobile regime than in the static regime at coalescence (0.28 ML). The associative O_2 sticking probability is high [from Fig. 2(a), ~0.17] on the (1×1) islands at $\theta_O=0.2$ ML. Thus, when the temperature is sufficiently high for rapid diffusion of O adatoms, a significant contribution to island growth occurs by the outdiffusion of adatoms from (1×1)-O islands to the surrounding (1×5) phase, maintaining a local (1×1)-O coverage of 0.2 ML. However, at low temperatures, when the adlayer is static, the coverage in the (1×1)-O islands increases by adsorption from the gas phase until, at a local coverage of 0.28 ML, the sticking probability on the (1×1)-O islands has dropped to 0.12, which is the same as the sticking probability on the (1×5) areas of the crystal: island growth therefore proceeds with an increasing local coverage, reaching 0.28 ML at coalescence.

A simple test for the onset of diffusion at temperatures above 600 K was conducted. The sticking probability dependence on coverage was measured at 350 K until the total coverage of 0.2 ML was achieved, corresponding to the local coverage during island growth at temperatures $\geqslant$700 K; this is shown as a grey line in Fig. 2(a). Adsorption was terminated at this point, and the adsorbed layer was annealed by heating the crystal to 800 K for 1 min before cooling to 350 K and restarting the oxygen adsorption. An increase in the sticking probability, by almost a factor of 2, was found, indicated by the vertical arrow in Fig. 2(a). Subsequent to annealing, the sticking probability curve had switched to the curve corresponding to the $\geqslant$700 K experiments. Clearly, after annealing at $\theta=0.2$ ML outdiffusion from the (1×1)-O islands, with an initial local coverage approaching 0.28 ML, has occurred, covering the whole surface and hence completing the $(1\times5)\rightarrow(1\times1)$ restructuring process, in support of a static-to-mobile switch in growth regimes between 600 and 700 K.

It would be useful to have direct measurements of the local coverages on the (1×5) substrate during the lifting of the reconstruction. In the coverage range from 0 to 0.04 ML the results may be attributed to adsorption on the (1×5) substrate up to a critical value where the adsorbate-induced restructuring can start. However, the TEAS results exhibit a flat plateaulike section in the coverage range 0–0.03 ML, which is attributed to adsorption on defect sites (Sec. III C). A defect concentration of up to 3% is quite possible, especially in view of the relatively low annealing temperature used (1400 K). Moreover, all attempts to determine the local oxygen coverage on the (1×5) surface during the phase transformation by lifetime measurements or isothermal desorption measurements, failed. We believe that this was due to a small difference in adsorption heats on the (1×1) and (1×5) phases for O_2 on Ir{100}.

C. LEED and TEAS during oxygen adsorption

LEED observations made simultaneously with sticking probability measurements showed that at 350 K the adsorbate-induced lifting of the (1×5) reconstruction (Fig. 1) produced a poorly ordered (1×1) Ir surface, with a high background intensity and some residual (1×5) beam intensity. The restructuring process is incomplete at this temperature. At 200 K, after saturation of the (1×5) surface with oxygen, the LEED pattern remained practically unchanged, except for some enhancement of the background intensity; the (1×5) structure is frozen in and the sticking probability drops to zero at coverages as low as 0.2 ML. The initial sticking probability on the (1×5) is 0.55, considerably higher than at temperatures $\geqslant$350 K. This is attributed to adsorption into a molecular dioxygen state on the (1×5) surface. In contrast, adsorption at temperatures above 700 K produces a good (1×1) LEED pattern, with low background intensity, even at 0.20 ML. As the coverage is increased from 0.04 to 0.20 ML the (1×5) diffraction features are continuously weakened and the integral order spots enhanced. On the (1×1) substrate near the saturation coverage (0.5 ML) a streaky (2×2) LEED pattern developed, which could be sharpened by annealing cycles close to the onset temperature for desorption, with additional oxygen dosing. Eventually a high quality (2×2) LEED pattern could be obtained. At 0.5 ML this is due to mixed domains of (2×1) symmetry.

The complete restructuring process involves a microscopic rearrangement of atomic positions, when isolated (1×1) islands are initially formed; the two surfaces differ in density by 15%. It also involves the macroscopic annealing of a surface consisting of many small coalescing islands, to establish long-range order in the first substrate layer. The limitation of long-range mass transport necessary for the formation of large (1×1) islands, due to the high barrier to self-diffusion for Ir atoms,[9] accounts for the lack of order in the (1×1) substrate after saturation of the surface with oxygen at 350–600 K, and explains the result that on Ir{100}-(1×5) even the nucleation of (1×1) island growth is inhibited at temperatures around 200 K.

To investigate structural changes of the substrate during the adsorption process, we performed He TEAS experiments simultaneously with sticking probability measurements using mixed He/O_2 beams. In Fig. 4, the absolute oxygen sticking probability and the relative He specular reflectivity are plotted vs total oxygen coverage. At $T_s=900$ K, the positions where the adsorbate-induced restructuring starts (0.05 ML) and is completed (0.20 ML) are marked by well-defined sharp breaks in the TEAS curve, indicating a sudden structural change of the substrate. In contrast the TEAS curve at 350 K, Fig. 5, exhibits an almost linear drop between 0.04 and 0.27 ML and no sharp changes in slope are observed. The TEAS curve during oxygen adsorption on the metastable (1×1) substrate (Fig. 5) exhibits a shape characteristic of random adsorption of oxygen adatoms.

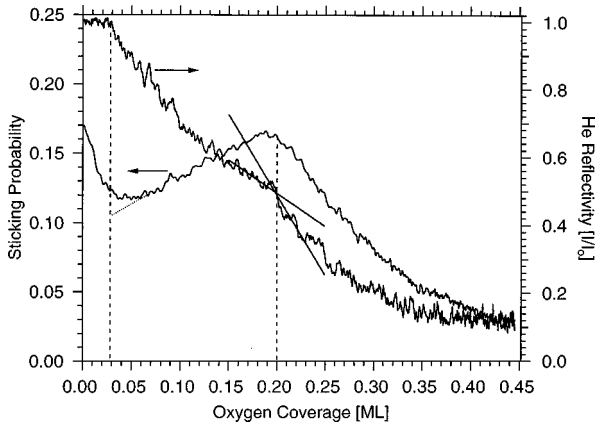

FIG. 4. Absolute sticking probability and He specular intensity vs oxygen coverage at 900 K. Beam flux: 0.008 ML/s, beam energy: 0.06 eV. The lines demonstrate the change of slope of the TEAS curve at 0.20 ML.

An attempt was made to explain the experimental TEAS intensity vs O-coverage curves (Fig. 5) by a simple island growth model, as described by Poelsema and Comsa.[29] A large cross section for He diffuse scattering from isolated adsorbed species results in the degree of overlap being strongly dependent on the adsorbate distribution. This is re-

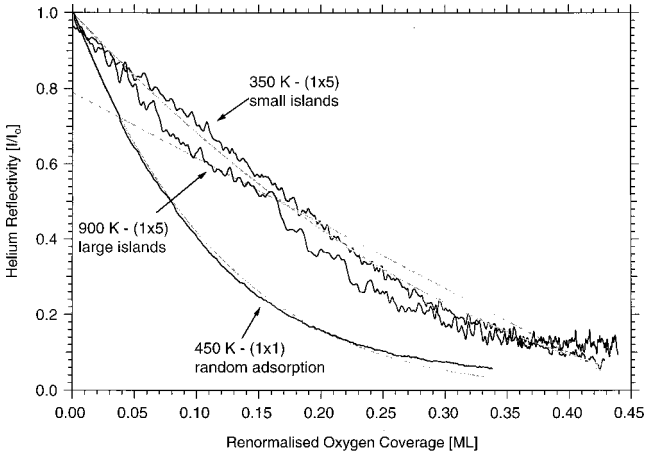

FIG. 5. Relative He specular intensity vs oxygen coverage starting with the clean (1×5) surface at 350 and 900 K and with the clean (1×1) at 450 K. The light grey curves represent a least-squares fit of the simple models for island formation and random adsorption as described in the text. The dashed lines show the change of slope in the 900 K experiment at the renormalized (see the text) coverage of 0.16 ML.

flected in the coverage dependence of the specular He peak height ratio (or reflectivity), I/I_0, where I_0 is the specular peak height reflected from the clean surface. For a random distribution, one obtains:

$$I/I_0=(1-\theta)^{n\Sigma}, \tag{2}$$

where θ is the fractional coverage, n is the number of surface atoms per unit area ($n=1.32\times10^{15}$ atoms/cm^2 for Ir{100}-(1×1)), and Σ is the total cross section for diffuse scattering. If the adsorbate forms islands and the islands are larger than the transfer width of the scattering instrument, then

$$I/I_0=1-nU\theta, \tag{3}$$

where U is the size of the unit cell in the islands. However, if the island sizes are small compared to the transfer width, the correct function is

$$I/I_0=(1-nU\theta)^2. \tag{4}$$

As discussed above, at low coverages (below 0.04 ML) adsorption takes place mostly at defect sites. Since an Ir atom defect *and* an O adatom at a defect scatter diffusely, there should be no change in He specular scattering intensity at $\theta\leqslant0.04$ ML, as actually observed (Fig. 4). To analyze the data above $\theta=0.05$ ML, it was therefore assumed that adsorption on the planar surface begins at 0.04 ML, and a relative scattering intensity of 1 was attributed to this surface. The coverage axis in Fig. 5 has therefore been renormalized (by subtracting 0.04) to exclude the influence of adsorption on defect sites. The light grey lines (Figs. 4 and 5) represent calculated TEAS intensities according to the simple expressions given above. A good fit is obtained for the random adsorption model on the clean metastable (1×1) surface; there is no island formation. In this case, the best fit revealed a scattering cross section of 62 Å^2. This value is higher than for oxygen adsorption on other surfaces, e.g., Ni{100}, where a value of 30 Å^2 was measured for oxygen atoms adsorbed in fourfold hollow sites.[30] A value of 40 Å^2 was measured by Guo *et al.* for O_a on the metastable Pt{100}-(1×1) surface.[20] We note that the recent density function theory (DFT) calculations to determine the preferred adsorption sites of O adatoms on Ir{100}-(1×1)[31] have shown that the bridge site is clearly energetically more favorable over the whole coverage range. Oxygen atoms adsorbed on bridge sites should have a higher scattering cross section compared to those in hollow sites. This supports the rather large value of 62 Å^2 determined from our experiments.

The 350 K experiment (Fig. 5) exhibits a linear drop of the specularly scattered intensity between (renormalized) coverages of 0 and 0.3 ML, indicating the formation of islands larger than the transfer width of our instrument. Under our measurement conditions, the value for the transfer width of the helium beam is estimated as 13 Å. A best fit of the linear model in the range of low coverages (Fig. 5) yielded a value of $U=21$ Å^2 for the area of the unit cell in the islands at $T_s=350$ K and of $U=30$ Å^2 at $T_s=900$ K. The formation of smaller islands at 900 K compared with those at 350 K is unlikely, and the linear model can be readily applied. The size of the substrate unit cell, U_{suc}, on Ir{100}-(1×1) is 7.3 Å^2. The ratio U_{suc}/U yields a local oxygen coverage of 0.35 ML on the growing (1×1) substrate at $T_s=350$ K and 0.24 ML at $T_s=900$ K. These values are higher than those derived from our sticking probability experiments, but the ratio of the local island coverages at 350 and 900 K is equal to the ratio of 0.28 and 0.20 ML local coverages derived from Fig. 2.

The TEAS intensities up to the (renormalized) coverage $\theta_r=0.1$ ML can be explained using different local coverages on the growing (1×1) domains, but above this coverage, in contrast to the 350 K experiment, the slope of the 900 K experiment flattens. Then, at a (renormalized) coverage of $\theta_r=0.16$ ML (=0.20–0.04), a sharp break is observed (the dashed lines in Fig. 5) and the slope becomes steeper again. This behavior is probably due to the formation of a uniform and well annealed (1×1) substrate at 900 K, at the point where the mean *total* coverage is 0.20 ML. As the substrate approaches structural perfection, the reflectivity decreases less steeply, although the mean O coverage still increases. Once a complete (1×1) surface has formed, further adsorption of oxygen occurs at random positions on the surface, as reflected by the curvature of the 900 K experiment at an *actual* coverage greater than 0.2 ML. Structural perfection is not established at $T_s=350$ K, and therefore no such break is seen in the TEAS experiment. Thus the TEAS results support the two mechanisms for island growth, at high and at low T_s, given in Sec. III B.

Finally, from Fig. 4 we can make an estimate of the dissociative sticking probability at zero coverage on a *defect-free* Ir{100}-(1×5) surface. We have demonstrated that the initial sharp fall in s at $\theta\leqslant0.03$ ML is due to adsorption on defects. Thus a linear extrapolation of the s vs θ plot back to $\theta=0.03$ ML (the dotted line in Fig. 4) produces the required value, $s=0.10\pm0.02$.

D. The growth rate power law

For the adsorption of CO[32] and D_2 [16] on Pt{100}-hex the rate of (1×1) island growth is accompanied by a strong flux dependence of the net sticking probability in the range of total coverages where the restructuring to (1×1) takes place at substrate temperatures of ~400 K for CO[15] and of ~240 K for D_2.[16] The key factor in determining this flux dependence is that it is observed at substrate temperatures where the lifetime of the adsorbate on the hex phase is short ($\leqslant$1 s) compared to the experimental time scale, and effectively infinite for adsorbate on the (1×1) phase. For O_2 on Ir{100}, we can anticipate that this temperature condition would be met at temperatures close to the onset of desorption of O_2 from Ir{100}(1×1)-O, at coverages $\leqslant$0.2 ML; from the results in Sec. III E, we predict that these conditions will be met at $T_s>900$ K. For oxygen adsorption on Ir{100}, we have concluded above that a similar *dynamic* mechanism becomes dominant at temperatures above 650 K. Complete restructuring to the (1×1) substrate can still be achieved during uptake at 1000 K using a flux of 0.007 ML/s. However, at 1080 K this flux is insufficient to lift the (1×5) reconstruction, since the O_2 desorption rate is high and the local oxygen coverage on the (1×5) substrate is too low to in-

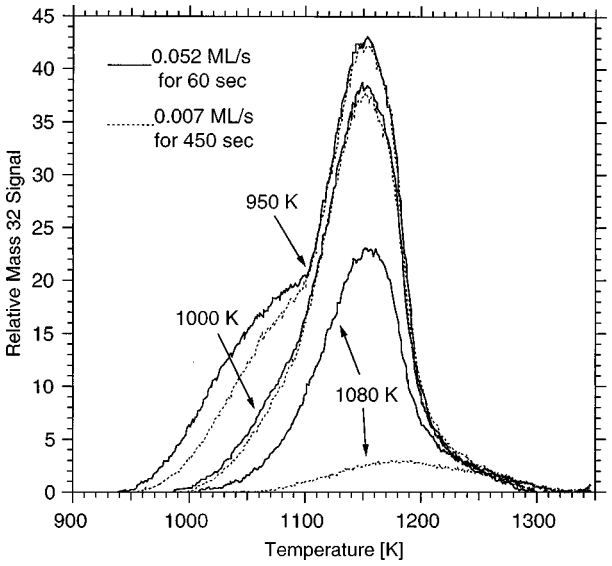

FIG. 6. TPD spectra obtained after equal exposures at two different fluxes (solid lines: 0.052 ML/s for 60 s; dotted lines: 0.007 ML/s for 450 s) at sample temperatures of 950, 1000, and 1080 K.

duce (1×1) island formation (Fig. 2). TPD spectra obtained after *equal exposures* to oxygen, but using different fluxes and exposure times, are shown in Fig. 6 for adsorption temperatures of 950, 1000, and 1080 K. The peaks represented by dashed lines are from 450 s, 0.007 ML/s exposures; the solid lines represent a 60 s, 0.052 ML/s exposure. Within experimental error, the TPD peak areas suggest that equal amounts of oxygen are adsorbed at 950 and at 1000 K for *both* exposures. The sticking probability is not flux dependent at these temperatures. This data also demonstrates the absence of clean-off reactions, e.g., with background CO, in these high temperature experiments. However, at 1080 K, and using the same exposures but different fluxes, it is found that the amount of adsorbed oxygen is 10 times higher if an 8 times higher flux is applied (Fig. 6). The flux dependence is clearly observed at this temperature. Sticking probability measurements at 1080 K at fluxes between 0.003 and 0.04 ML/s are shown in Fig. 7(a). The results are strongly reminiscent of the data of Hopkinson *et al.*[15] for CO adsorption at 400 K. The shape of the $s(\theta)$ curve at the highest flux is very similar to the ''high temperature'' series in Fig. 2; the lower saturation coverage is readily attributed to desorption from the (1×1)-O surface as the coverage proceeds beyond 0.2 ML.

Figure 7(b) shows the dependence of the specular He intensity on exposure at 1080 K, under the same conditions as the data in Fig. 7(a). This result confirms that desorption from (1×1)-O makes no significant contribution to the observed flux-dependent sticking probability at $\theta<0.20$ ML. At exposures greater than ~0.5 ML, at equal exposures and different fluxes, different TEAS intensities are observed, in agreement with the sticking probability data.

To determine the power law for the $(1\times5)\rightarrow(1\times1)$ oxygen-induced process, we require a knowledge of the local O(ad) coverage on the (1×5) surface during the phase transformation at 1080 K, and its dependence on the flux. We were unable to obtain desorption spectra for O_2 from the

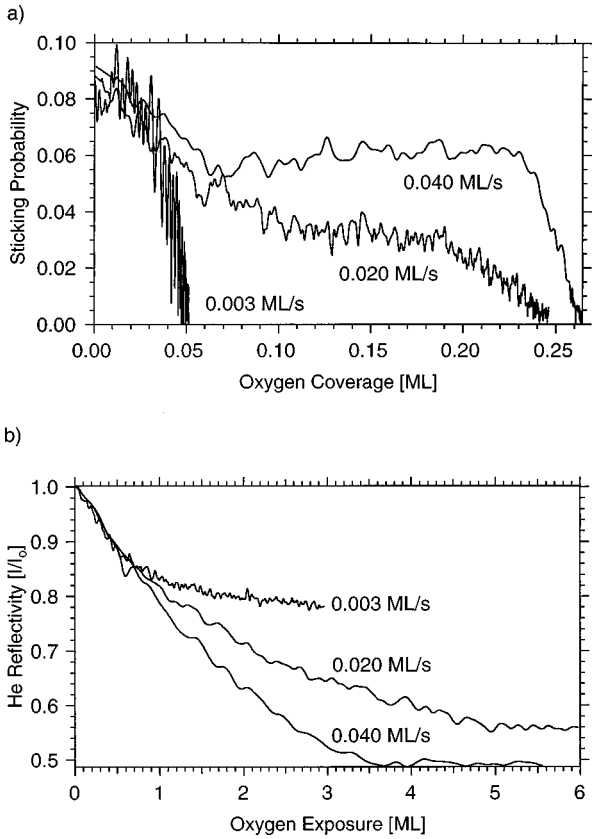

FIG. 7. (a) Sticking probability vs oxygen coverage at 1080 K sample temperature for three different fluxes. (b) He specular intensity measured simultaneously with the oxygen adsorption as function of total oxygen exposure.

unreconstructed (1×5) surface: TPD spectra after adsorption at 200 K on the (1×5) phase (with no lifting of the reconstruction) yield desorption from the (1×1) surface, because in the temperature range 350–1000 K, leading to the onset of desorption, oxygen initially adsorbed on the (1×5) restructures the surface and becomes trapped in growing (1×1) islands or defect sites. Attempts to measure O adsorbate lifetimes, and thus coverages, at high temperatures failed due to the presence of a high density of defect sites.

An alternative route to the power law is obtained by assuming a simple, low coverage Langmuir expression for dissociative adsorption, relating the oxygen partial pressure P_{O_2} to the adatom coverage on the (1×5) phase, $\theta_O^{1\times5}$:

$$\theta_O^{1\times5}=k\sqrt{P_{O_2}}. \tag{5}$$

If the (1×1) island growth rate dependence on the adatom coverage on the (1×5) areas of the surface, $\theta_O^{1\times5}$, is

$$r_{1\times1}=c(\theta_O^{1\times5})^n, \tag{6}$$

n can be estimated as follows. For dissociative adsorption, and switching to *flux* dependence, Q,

$$\frac{dN_{1\times1}}{dt}=c'Q^{n/2}; \tag{7}$$

changing from time to exposure, Ex, where $\mathrm{Ex}=Qt$, gives

$$\frac{dN_{1\times1}}{d\mathrm{Ex}} = c' Q^{n/2}/Q = c' Q^{n/2-1}. \tag{8}$$

For relatively low exposures, it can be assumed that there is no change in the adsorption rate with exposure, hence

$$N_{1\times1} = c' Q^{n/2-1}\mathrm{Ex}. \tag{9}$$

Thus, for two different exposures,

$$(N_{1\times1})'/(N_{1\times1})'' = (Q'/Q'')^{n/2-1}. \tag{10}$$

Using Eq. (10) it is possible to determine a value for n from TPDs obtained after dosing for a constant exposure using two different fluxes. With this method, and the oxygen TPDs at 1080 K (fluxes 0.052 and 0.007 ML/s) shown in Fig. 6, we obtain a reaction order $n=3.6$ in the power law expression for O_2 adsorption on Ir{100}. This value may be an underestimation since it remains unclear what fraction of the TPD at 1080 K (Fig. 6) can be attributed to desorption from defect sites.

The sticking versus coverage curves in Fig. 7(a) provide an additional possibility for estimating the apparent reaction order. A method for the determination of the local CO coverage on Pt{100}-hex during the restructuring to (1×1) is described in Ref. 15. The desorption rate r_d from the (1×5) substrate can be derived for any total coverage of O(ad) from the difference of the sticking probabilities with and without desorption, i.e., net and absolute sticking:

$$r_d = Q(s_a - s_n). \tag{11}$$

The value for the absolute adsorption rate, Qs_a, can be derived from the average sticking probability in Fig. 2 at 0.06 ML, since this is not influenced by desorption during uptake. The (1×1) island growth rate at any total oxygen coverage is given by

$$r_{(1\times1)} = Qs_n. \tag{12}$$

This method can also be applied for dissociative adsorption. In this case the local oxygen coverage on the Ir{100}-(1×5) surface is derived from the square root of the desorption rate, r_d, which can be determined from the sticking probability versus coverage profiles. The break at 0.06 ML in Fig. 7(b) corresponds to the onset of the oxygen-induced restructuring, and at this coverage hardly any (1×1) has been formed. Thus it is a reliable coverage for an estimation of the reaction order. Since the initial sticking probability is independent of T_s, at $\theta=0.06$ ML, $s_a=0.22$ (Fig. 2). The net sticking probability is obtained by taking a linear fit of the data points (Fig. 7) in the coverage range 0.06–0.19 ML, i.e., within the plateaulike section of the experiments, in order to read the average values. The net sticking probabilities at 0.06 ML are 0.06 and 0.03 for fluxes of 0.04 and 0.02 ML/s, respectively. Hence, for a flux of 0.04 ML/s, it follows from Eqs. (11) and (12), that

$$\theta_{\mathrm{O}}^{1\times5} = \sqrt{r_d} = 0.08, \quad r_{1\times1} = 0.0024 \ \text{ML/s}.$$

Similarly, for the 0.02 ML/s flux, $\theta_{\mathrm{O}}^{1\times5}=0.06$ ML/s, and $r_{1\times1}=0.0008$ ML/s. Substituting these values into the power law expression, Eq. (6), reveals values of $n=5.3$ and $c=1.6\times10^3\ \mathrm{s}^{-1}$.

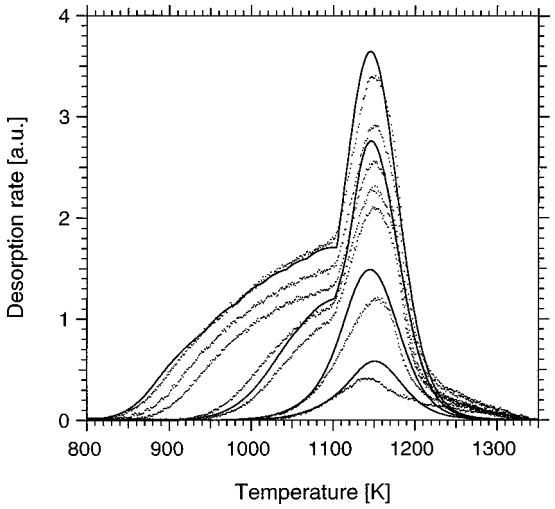

FIG. 8. Experimental TPD spectra (dotted lines) for O_2 dosed onto an initially clean Ir{100}-(1×5) surface. The exposures were between 0.81 and 72.9 ML, yielding coverages of 0.04–0.5 ML. Adsorption was carried out at 500 K; the linear heating rate was 4.0 K/s. Modeled (solid lines) TPD spectra are also shown.

We conclude that the two estimations of n show that a strongly nonlinear process is operative for oxygen-induced lifting of the (1×5) reconstruction of the Ir{100} surface, with $n=4.5\pm1$.

E. Thermal desorption measurements

Figure 8 shows a series of TPD spectra after exposures between 0.8 and 73 ML on the initially clean (1×5) surface. The sample temperature during adsorption was 500 K. At the highest initial coverage of 0.5 ML, the desorption rate increases slowly over a wide temperature range (820–1100 K). This is followed by a sharp break where a steep increase of the desorption rate takes place. Integration of the TPD up to this break yields a remaining oxygen coverage of 0.25 ML. On the sticking probability curves (Fig. 2) this coverage is close to the position of the sharp break assigned to the end of the adsorbate-induced restructuring and the formation of a complete (1×1) substrate. Accordingly, desorption between 820 and 1100 K takes place from the Ir{100}-(1×1) surface. This result is confirmed by sequential LEED observations obtained by terminating the temperature ramp at specified remaining O coverages. These show that fractional order spots of the reconstructed (1×5) surface are detected at residual coverages below 0.20 ML.

The TPD spectra starting at coverages between 0.5 and 0.21 ML exhibit very similar shapes to the 0.5 ML experiment, the only difference being that the onset of desorption is successively shifted to higher temperature; the temperature at the steep desorption rate increase is unchanged, at 1100 K, for all spectra. The peak temperature, T_p, is very slightly shifted up, by a few degrees. For coverages lower than 0.21 ML the desorption peaks are at constant T_p (1150 K) and halfwidth, consistent with desorption from contracting (1×1) islands.

The role of defects can be estimated from the TPD spectrum from an initial oxygen coverage of ~0.12 ML, Fig. 8.

A shoulder is apparent with $T_p = 1230$ K, about 80 K higher than the peak temperature of the main peak. The area corresponding to this peak indicates a coverage of about 0.03 ML, which is close to the coverage of defect sites deduced from the sticking probability (Fig. 2) and TEAS (Fig. 4) data.

IV. MATHEMATICAL MODEL

Our model of the associative desorption of O_2 from Ir{100} is based on the following reaction steps:

(A) $2O_{1\times1} \rightarrow O_{2(g)} + 2^*_{1\times1}$,
(B) $2O_{1\times5} \rightarrow O_{2(g)} + 2^*_{1\times5}$,
(C) $O_{1\times1} \leftrightarrow O_{1\times5}$,
(D) $1\times1 \rightarrow 1\times5$.

$^*_{(1\times1)}$ and $^*_{(1\times5)}$ denote a free adsorption site on the (1×1) and the (1×5) substrate, respectively. Step (C) represents the interdiffusion of oxygen between (1×1) and (1×5), i.e., trapping and untrapping. Step (D) represents the (1×1) to (1×5) phase transition. Taking second-order desorption kinetics for oxygen into account for both (1×1) and (1×5) surfaces, the following set of coupled differential equations describes the change of oxygen coverage on (1×5) and (1×1) and the change in the fraction of (1×1) surface, $\theta_{(1\times1)}$. The oxygen coverage refers to the respective local coverage on the two phases and is expressed in monolayers (ML) relative to the iridium atom density in the ideal (1×1) surface,

$$\frac{d\theta_O^{1\times1}}{dt} = -k_1(\theta_O^{1\times1})^2 + k_3\frac{\theta_O^{1\times5}}{\theta_{1\times1}}B - k_4\frac{\theta_O^{1\times1}}{\theta_{1\times1}}B - \frac{\theta_O^{1\times1}}{\theta_{1\times1}}\frac{d\theta_{1\times1}}{dt}, \tag{13}$$

$$\frac{d\theta_O^{1\times1}}{dt} = -k_2(\theta_O^{1\times5})^2 - k_3\frac{\theta_O^{1\times5}}{\theta_{1\times5}}B + k_4\frac{\theta_O^{1\times1}}{\theta_{1\times5}}B - \frac{\theta_O^{1\times5}}{\theta_{1\times5}}\frac{d\theta_{1\times1}}{dt}, \tag{14}$$

where

$$\frac{d\theta_{1\times1}}{dt} = -k_5\left(1 - \frac{\theta_O^{1\times1}}{\theta_O^{crit}}\right)\theta^{1\times1} \quad \text{if} \quad \frac{\theta_O^{1\times1}}{\theta_O^{crit}} < 1. \tag{15}$$

The last term in the rate equations is required to maintain mass balance of the adsorbate as $\theta_{(1\times1)}$ changes.

Table I describes the terms used in the above rate equations, as well as the values used for the different parameters in the model. The coverage dependence of the oxygen desorption energy from the (1×1) phase was determined empirically, by fitting to the TPD spectrum at $\theta = 0.5$ ML. This coverage dependence can be approximated with $E_d = (336 - 216\theta^2)$ kJ/mol.

The calculated desorption spectra based on the above model are shown in Fig. 8 as the solid lines, along with the experimental TPD data (the dashed curves). The peak shape at coverages below 0.25 ML is strongly influenced by the rate of the phase change and the difference in binding energies of oxygen on the (1×5) and (1×1) substrates. Using a higher rate for the phase change and a higher desorption rate from the (1×5) was very effective in causing the overall desorption rate at 0.25 ML to become steeper as well as in shifting the position of the peak maximum to high temperatures. An optimum fit was obtained with a difference in the oxygen desorption energy from the different substrates of ~40 kJ/mol and a preexponential for rate of the phase change of 2×10^2 s^{-1}. An activation barrier of 84.9 kJ/mol for the reconstruction was taken from literature.[2,4] Surprisingly, this is lower than the corresponding value of 106 kJ/mol for the similar restructuring process of Pt{100}-(1×1) (the kinetic phase transformation takes place at about *twice* the temperature); the result is a small value for the preexponential. The only major deviation from the experimental curve occurs at temperatures above 1200 K, due to desorption from strongly bound oxygen on defect sites not accounted for in the model.

TABLE I. Parameters used to model the oxygen TPDs.

Description	Parameter	E_a (kJ mol^{-1})	ν(s^{-1})
Desorption (1×1)	k_1	$\theta<0.28$: $E_1=337$ $\theta\geqslant0.28$: $E_1=356-216\theta^2$	2.0×10^{14}
Desorption (1×5)	k_2	$E_2=160$	2.0×10^{10}
Trapping	k_3	0	$k_4\nu_2 s_{1\times1}/\nu_5 s_{1\times5}$
Untrapping	k_4	E_1-E_2	1.0×10^4
$(1\times1)\rightarrow(1\times5)$	k_5	84.9	2.0×10^2
Sticking on (1×1)	$s_{1\times1}=0.25$		
Sticking on (1×5)	$s_{1\times5}=0.12$		
(1×1) boundary length	$B=1$		
Critical coverage	$\theta_O^{crit}=0.25$		

Studies of the kinetics of the $(1\times1)\rightarrow(1\times5)$ clean surface transformation on Ir{100} have revealed a deviation from simple activated restructuring kinetics in the final stages of the process.[2,3] The completion of the phase change is slow because long-range order in the reconstructed (1×5) substrate has to be established, involving a mesoscopic scale rearrangement of nonmatching hex patches. According to Heinz *et al.* sample temperatures above 1300 K are necessary to make this process sufficiently fast.[2,3]

V. CONCLUSIONS

The interaction of oxygen with the stable Ir{100}-(1×5) and the metastable (1×1) surfaces has been studied using supersonic molecular beams in the surface temperature range 200–1080 K. The initial sticking probability for oxygen on a defect-free Ir{100}-(1×5) surface is estimated as 0.10 ± 0.02 and on (1×1) it is 0.24 ± 0.02.

The oxygen induced lifting of the (1×5) reconstruction results from the nucleation, mainly at defect sites, and subsequent growth of (1×1) islands. Thermal energy atom scattering (TEAS) and sticking probability data have revealed two distinct temperature regimes in this process; the lifting of the reconstruction occurs over the coverage range 0.05–0.28 ML for the low substrate temperature regime (350–600 K), and from 0.05 to 0.20 ML at between 700 and

1000 K. At all temperatures, island growth of the (1×1) is initiated at $\sim$0.05 ML. These two regimes are accounted for by an enhancement of surface diffusion of oxygen adatoms at sample temperatures around 650 K. Below this temperature, the low mobility of O(ad) is responsible for random occupation of free adsorption sites on the (1×1) islands, and the excess O atoms are not available for the formation of additional (1×1) area. However, at sample temperatures exceeding 650 K, internal equilibrium with respect to the distribution of the adsorbate on both (1×5) and (1×1) domains is achieved very rapidly.

The formation of (1×1) islands, with a local coverage of 0.28 ML at sample temperatures below 650 K and with 0.20 ML at higher temperatures, has also been demonstrated by TEAS. In contrast to the (1×5) phase, random adsorption of O_2 is observed on the clean metastable (1×1) surface.

It has been found that, at 1080 K, the rate of Ir{100}-(1×1) island growth has a strongly nonlinear dependence on the local oxygen coverage on the (1×5) domains. This nonlinearity manifests itself in a strongly flux-dependent sticking probability in the range of total coverages where the restructuring toward (1×1) takes place. The average apparent reaction order of $n=4.5$, determined from two different methods, for this process is surprisingly similar to that found previously for CO and D_2 on Pt{100}.

TPD and LEED observations indicate that the rate of desorption of oxygen from Ir{100}-(1×1) is strongly enhanced at temperatures where the major structural transition from $(1\times1)\rightarrow(1\times5)$ takes place; repulsive lateral interactions exist between adsorbed oxygen atoms on the (1×1) substrate. A mathematical model has been used to successfully describe the main features of the TPD spectra.

ACKNOWLEDGMENTS

We acknowledge the Oppenheimer Trust for a research studentship (T.A.), the FWF, Vienna, for an Erwin Schrödinger Scholarship (B.K.), Shell Research and Technology Centre, Amsterdam for a studentship (A.V.W.), and the EPSRC for an equipment grant. We are grateful to Victor Ostanin for helpful discussions and for technical support.

[1] A. Ignatiev, A. V. Jones, and T. N. Rhodin, Surf. Sci. **30**, 573 (1972).
[2] K. Heinz, G. Schmidt, L. Hammer, and K. Müller, Phys. Rev. B **32**, 6214 (1985).
[3] N. Bickel and K. Heinz, Surf. Sci. **163**, 435 (1985).
[4] J. Küppers and H. Michel, Appl. Surf. Sci. **3**, 179 (1979).
[5] M. A. van Hove, R. J. Koestner, P. C. Stair, J. P. Biberian, L. L. Kesmodel, I. Bartos, and G. A. Somorjai, Surf. Sci. **103**, 189 (1981).
[6] T. N. Rhodin and G. Broden, Surf. Sci. **60**, 466 (1976).
[7] Q. Ge, D. A. King, N. Marzari, and M. Payne, Surf. Sci. (submitted).
[8] G. Kisters, J. G. Chen, S. Lehwald, and H. Ibach, Surf. Sci. **245**, 65 (1991).
[9] G. Boisvert, L. J. Lewis, M. J. Puska, and R. M. Nieminen, Phys. Rev. B **52**, 9078 (1995).
[10] T. Ali, B. Klötzer, A. V. Walker, and D. A. King, J. Chem. Phys. (submitted).
[11] J. T. Grant, Surf. Sci. **18**, 228 (1969).
[12] J. U. Mack, E. Bertel, F. P. Netzer, and D. R. Lloyd, Z. Phys. B **63**, 97 (1986).
[13] C. B. Mullins, Y. Wang, and W. H. Weinberg, J. Vac. Sci. Technol. A **7**, 2125 (1989).
[14] S. Titmuss, A. Wander, and D. A. King, Chem. Rev. **96**, 1291 (1996).
[15] A. Hopkinson, X. C. Guo, J. M. Bradley, and D. A. King, J. Chem. Phys. **99**, 8262 (1993).
[16] A. T. Pasteur, St. J. Dixon-Warren, and D. A. King, J. Chem. Phys. **103**, 2251 (1995).
[17] M. Gruyters, T. Ali, and D. A. King, Chem. Phys. Lett. **232**, 1 (1995).
[18] M. Gruyters, A. T. Pasteur, and D. A. King, J. Chem. Soc., Faraday Trans. **92**, 2941 (1996).
[19] A. V. Walker, M. Gruyters, and D. A. King, Surf. Sci. **384**, L791 (1997).
[20] X. C. Guo, J. M. Bradley, A. Hopkinson, and D. A. King, Surf. Sci. **310**, 163 (1994).
[21] J. M. Bradley, X. C. Guo, A. Hopkinson, and D. A. King, J. Chem. Phys. **104**, 4283 (1996).
[22] A. Hopkinson, Ph.D. thesis, University of Cambridge, 1993.
[23] P. Gardner, R. Martin, R. Nalezinski, C. L. A. Lamont, M. J. Weaver, and A. M. Bradshaw, J. Chem. Soc., Faraday Trans. **91**, 3575 (1995).
[24] P. R. Norton, P. E. Bindner, and K. Griffiths, J. Vac. Sci. Technol. A **2**, 1028 (1984).
[25] D. A. King and M. G. Wells, Surf. Sci. **29**, 245 (1972).
[26] J. K. Fremerey, J. Vac. Sci. Technol. A **3**, 1715 (1985).
[27] D. A. King and M. G. Wells, Proc. R. Soc. London, Ser. A **339**, 245 (1974).
[28] A. Borg, A. M. Hilmen, and E. Bergene, Surf. Sci. **306**, 10 (1994).
[29] C. Poelsema and G. Comsa, *Scattering of Thermal Energy Atoms* (Springer, Berlin, 1989).
[30] J. Ibanez, N. Garcia, and J. M. Rojo, Phys. Rev. B **28**, 3164 (1983).
[31] Q. Ge and D. A. King (unpublished).
[32] A. Hopkinson, J. M. Bradley, X. C. Guo, and D. A. King, Phys. Rev. Lett. **71**, 1597 (1993).